

The thermopower of superconducting  $\text{Na}_x\text{CoO}_2 \cdot \gamma\text{H}_2\text{O}$ ; evidence for conduction in a very narrow band

This article has been downloaded from IOPscience. Please scroll down to see the full text article.

2003 J. Phys.: Condens. Matter 15 L571

(<http://iopscience.iop.org/0953-8984/15/37/L03>)

View [the table of contents for this issue](#), or go to the [journal homepage](#) for more

Download details:

IP Address: 171.66.16.125

The article was downloaded on 19/05/2010 at 15:10

Please note that [terms and conditions apply](#).

## LETTER TO THE EDITOR

## The thermopower of superconducting $\text{Na}_x\text{CoO}_2 \cdot \gamma\text{H}_2\text{O}$ ; evidence for conduction in a very narrow band

**B Fisher, K B Chashka, L Patlagan, A Kanigel, A Knizhnik,  
G Bazalitsky and G M Reisner**

Physics Department and Crown Centre for Superconductivity, Technion, Haifa 32000, Israel

Received 21 July 2003

Published 8 September 2003

Online at [stacks.iop.org/JPhysCM/15/L571](http://stacks.iop.org/JPhysCM/15/L571)

### Abstract

The absolute thermopower ( $S$ ) of superconducting  $\text{Na}_x\text{CoO}_2 \cdot \gamma\text{H}_2\text{O}$  is p-type. It increases superlinearly with temperature up to  $\sim 50$  K; at higher temperatures its rate of change decreases and saturation at  $S \approx 40 \mu\text{V K}^{-1}$  is observed above 150 K.  $S(T)$  for  $\text{Na}_x\text{CoO}_2 \cdot \gamma\text{H}_2\text{O}$  resembles that of anhydrous  $\text{Na}_x\text{CoO}_2$  ( $x \approx 0.7$ ), but is lower by a factor of  $\sim 2$  and its saturation is more pronounced. These results are consistent with electronic transport by strongly correlated electrons in a *very narrow band*.

The search for superconductivity in non-cuprate 3d transition metal oxides, led to the discovery of large thermopower in the highly conducting compound  $\text{Na}_x\text{CoO}_2$  [1]. Its crystal structure consists of a single layer of Na ions sandwiched between  $\text{CoO}_2$  layers with the Co ions located on the sites of a triangular lattice. It is paramagnetic with inverse magnetic susceptibility  $\chi^{-1} \propto (T + \theta)$  ( $\theta = +55 \pm 5$  K) [2]. This implies the existence of antiferromagnetic coupling below  $T = \theta$ , but because the spins form a triangular lattice, the antiferromagnetism is frustrated<sup>1</sup> [3].

Superconductivity below 5 K was discovered in  $\text{Na}_x\text{CoO}_2 \cdot \gamma\text{H}_2\text{O}$  ( $x = 0.35$ ) obtained by the partial extraction of Na from the parent compound,  $\text{Na}_{0.7}\text{CoO}_2$ , followed by intercalation of water [4]. The  $c$ -axis of the new compound is larger by a factor of 1.8 than that of the parent compound while the in-plane Co–Co distances remain almost unchanged.  $\chi$  of  $\text{Na}_x\text{CoO}_2 \cdot \gamma\text{H}_2\text{O}$  is more complicated, but it contains a term  $\propto (T + \theta)^{-1}$  with  $\theta = 37.6$  K [5]. This system provides a rare opportunity for studying electronic transport in a layered system where the interlayer distance undergoes a large change. The band filling governed by the Na content also changes. This work is devoted to the study of the effect of the structural (and band-filling) changes on the thermopower of the  $\text{CoO}_2$  layers. It shows that the main effect of these changes is a dramatic narrowing of the conduction band.

<sup>1</sup> A transition to a weak ferromagnetic order was detected at 22 K in a sample with  $x = 0.75$ , synthesized by a special technique.

**Table 1.** Na/Co ratio ( $x$  in  $\text{Na}_x\text{CoO}_2 \cdot \gamma\text{H}_2\text{O}$ ) obtained by EDS for samples of runs using different  $\text{Br}_2/\text{Na}_{0.7}\text{CoO}_2$  molar ratios and various molar concentrations of  $\text{Br}_2$  in  $\text{CH}_3\text{CN}$ .

| Intercalation run | $\text{Br}_2/\text{Na}_{0.7}\text{CoO}_2$ | $\text{Br}_2$ concentration | Na/Co       |
|-------------------|---|-----------------------------|-------------|
| A                 | 3.5                                       | 4.8                         | 0.276–0.290 |
| B                 | 3.5                                       | 2.3                         | 0.302–0.314 |
| C <sup>a</sup>    | 2.1                                       | 2.8                         | 0.393–0.395 |
| D                 | 30  | 14                          | 0.268–0.274 |
| E <sup>b</sup>    | 7.0                                       | 6.4                         |             |

<sup>a</sup> XRD shows presence of  $\text{Na}_x\text{CoO}_2$ .

<sup>b</sup> Prepared after the EDS session.

Polycrystalline samples of  $\text{Na}_x\text{CoO}_2$  with various nominal  $x$  were prepared by the conventional solid state reaction [6] from mixtures of Co and  $\text{Na}_2\text{CO}_3$ . All samples were characterized by x-ray diffraction (XRD) using a Siemens D5000 powder diffractometer with Cu  $K\alpha$  radiation. The XRD patterns for  $x = 0.6$ – $0.8$  indicated that these were monophasic materials.  $\text{Na}_x\text{CoO}_2 \cdot \gamma\text{H}_2\text{O}$  samples were prepared as in [4] from  $\text{Na}_{0.7}\text{CoO}_2$ , in several intercalation runs (A–E) using different solutions of  $\text{Br}_2$  in  $\text{CH}_3\text{CN}$  (see table 1). The XRD patterns for most samples of runs A, B, D and E showed no foreign phases; for the run C powder it showed the presence of a copious amount of unreacted  $\text{Na}_x\text{CoO}_2$ .

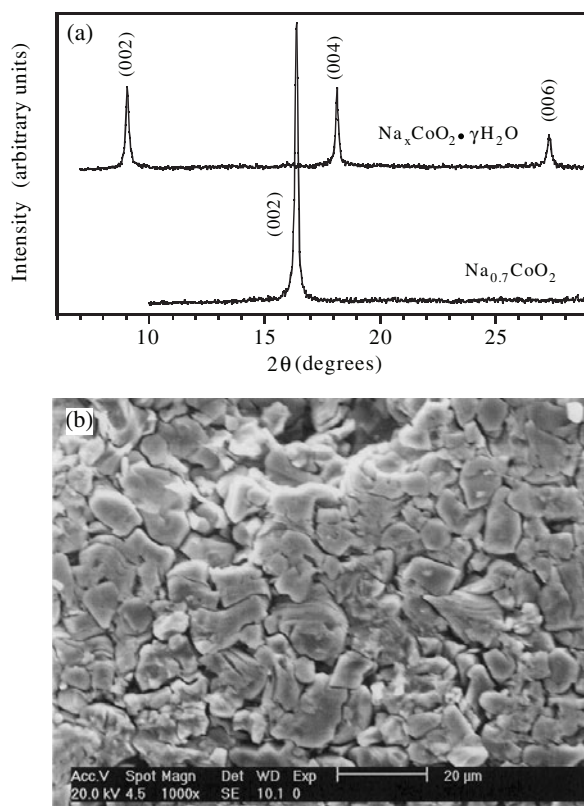
The Na/Co ratio ( $x$ ) of the samples from the A–D runs was obtained from energy dispersive spectroscopy (EDS) using a Philips XL30 SEM machine. The analyses were carried out on two well separated spots on the surface of each sample. The pair of  $x$  values for the various samples is shown in table 1. The difference between the two values of  $x$  for each sample is of the order of the maximal error of the machine ( $\pm 1$  at.% in determining the Co and Na contents)<sup>2</sup>. The large Na/Co ratio in C is apparently caused by the presence of unreacted  $\text{Na}_x\text{CoO}_2$ . The picture in the lower panel of figure 1 was taken of a sample from run B by the SEM during the same session.

Figure 1(a) represents the XRD pattern of a fresh  $\text{Na}_x\text{CoO}_2 \cdot \gamma\text{H}_2\text{O}$  sample (run A) and of its parent compound  $\text{Na}_{0.7}\text{CoO}_2$ . The lattice parameters of the hydrated sample were determined by least-squares fitting of the reflection peaks in the range of  $10^\circ \leq 2\theta \leq 140^\circ$  collected by step scan ( $0.03^\circ$  per 2 s step). They are:  $a = 2.823(1)$  Å and  $c = 19.624(7)$  Å, in good agreement with those reported in [4]. Repeated scans following long exposure of the hydrated samples to ambient atmosphere showed a decrease in the intensity of the 00l lines relative to the background, indicating an increase in the amount of amorphous material.

The temperature dependence of the (four-probe) resistivity  $\rho$  and thermopower  $S$  of cold-pressed samples of  $\text{Na}_x\text{CoO}_2 \cdot \gamma\text{H}_2\text{O}$  and of sintered samples of the parent material are shown in figures 2(a) and (b), respectively. Note that the scale of the left axis in figure 2(a) (for the hydrated samples) is one order of magnitude higher than that of the right axis (for the anhydrous sample).  $\rho(T)$  for the  $\text{Na}_{0.7}\text{CoO}_2$  sample agrees with corresponding plots in the literature. Plots A11 and A12 represent measurements on sample A1 carried out before and after ageing of several weeks;  $\rho$  has increased by about a factor of four and the temperature dependence has also changed. The intermediate plot (A2) represents another fresh sample from this batch. At low temperatures,  $\rho(T)$  has a negative coefficient of temperature indicating disorder in the grain-boundary layer. This layer seems to expand with the time of exposure to ambient pressure.

The reproducibility and stability of  $S(T)$  of the hydrated samples is in strong contrast with the irreproducibility and instability of its  $\rho(T)$ . All  $S(T)$  plots of these samples shown

<sup>2</sup> EDS analyses of the surfaces of the  $\text{Na}_x\text{CoO}_2$  samples, monophasic according to XRD, gave irreproducible Na/Co ratios (mostly larger than 1).



**Figure 1.** (a) XRD powder patterns of  $\text{Na}_x\text{CoO}_2 \cdot \gamma\text{H}_2\text{O}$  (upper trace) and  $\text{Na}_{0.7}\text{CoO}_2$  (lower trace). (b) A SEM picture of a sample of batch B.

in figure 2(b) are very close; while A3 and A4 were aged samples, B was a fresh one. The lowest plot is for a sample from the D run (lowest Na/Co ratio). The plot for an E sample (not shown) lies slightly above it. The insensitivity of the thermopower to grain boundaries has been emphasized in the past few decades; however, its robustness in this problematic material (cold pressed and sensitive to the atmosphere) is surprising<sup>3</sup>.

The DC magnetization plots of fresh powder from the B and E runs are shown in the inset of figure 2(b). These indicate transitions to superconductivity at  $T_c > 3$  K. For the powder from run D (lowest Na/Co ratio and lowest  $S$ )  $T_c < 1$  K.

Also shown in figure 2(b) is  $S(T)$  for  $\text{Na}_{0.7}\text{CoO}_2$  (using the right  $S$  axis). The plots for  $x = 0.6$  and  $0.8$  (not shown) lie slightly below and above that of  $x = 0.7$ . These results are in good agreement with earlier publications for poly- and single crystals of  $\text{Na}_x\text{CoO}_2$  [2, 6, 7].  $S(T)$  for the  $\text{Na}_x\text{CoO}_2 \cdot \gamma\text{H}_2\text{O}$  samples resemble that of  $\text{Na}_{0.7}\text{CoO}_2$  but are lower. The two types of plots are characterized by a steep rise with temperature at low  $T$  followed by a tendency towards saturation at high  $T$ . The saturation is much faster for  $\text{Na}_x\text{CoO}_2 \cdot \gamma\text{H}_2\text{O}$ . *Saturation of  $S(T)$  is the hallmark of a narrow band.* Figure 2(b) emphasizes the band narrowing on going from the anhydrous to the hydrated compound.

<sup>3</sup> Sintered  $\text{Na}_x\text{CoO}_2$  was crushed and cold pressed.  $S(\text{RT})$  measured prior to crushing and after compaction were identical. The resistivity of the granular sample was an order of magnitude larger than that of a sintered sample from the same batch.

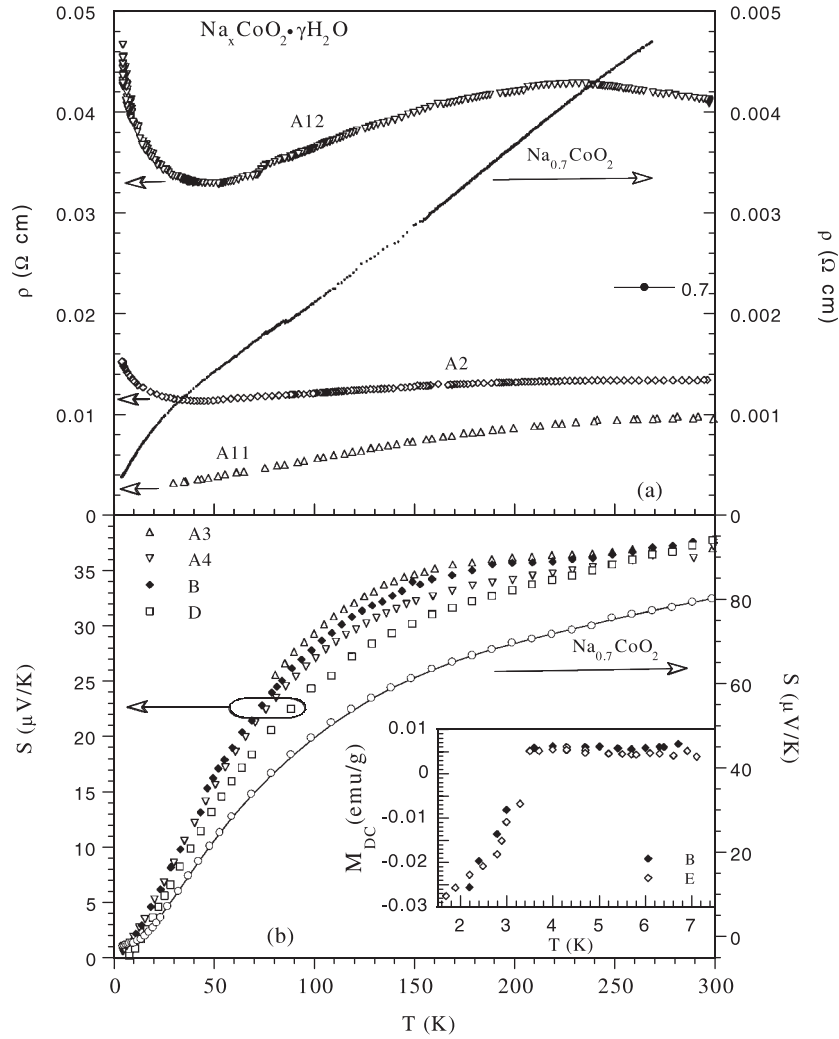


**Figure 2.** (a)  $\rho$  versus  $T$  for two samples of  $\text{Na}_x\text{CoO}_2 \cdot \gamma\text{H}_2\text{O}$  (A1 and A2) and a sample of the parent material  $\text{Na}_{0.7}\text{CoO}_2$ . The A11 and A12 data were measured on sample A1 fresh and after its long exposure to ambient atmosphere, respectively. (b)  $S$  versus  $T$  for samples of  $\text{Na}_x\text{CoO}_2 \cdot \gamma\text{H}_2\text{O}$  (upper traces, left  $S$  axis) and a sample of  $\text{Na}_{0.7}\text{CoO}_2$  (lower trace, right  $S$  axis). Magnetization versus  $T$  for two samples is shown in the inset of (b).

The thermopower of  $\text{Na}_x\text{CoO}_2$ , unusually large for a metal with high conductivity, has received various interpretations based on the standard transport theory for normal metals [8] on the one hand, and on strongly correlated carriers [9] on the other.

According to the standard transport theory, the absolute thermopower for carriers in a single, non-degenerate band (neglecting anisotropy) may be expressed as [10–12]:

$$S = \frac{1}{|e|T\sigma} \int_0^W \sigma(E)(\mu - E)(-\partial f/\partial E) dE, \quad (1)$$

where  $f$  is the Fermi distribution function,  $\mu$  is the chemical potential, the conductivity  $\sigma = \int_0^W \sigma(E)(-\partial f/\partial E) dE$ ,  $\sigma(E)$  is the low temperature conductivity if  $E_F$  was at  $E$  and

$W$  is the bandwidth. To the lowest order in  $k_B T/|E_F|$  ( $E_F$  measured from the bottom or from the top of the band), equation (1) becomes [10]:  $S = (\pi^2 k_B^2 T/3eE_F)(\partial \ln \sigma(E)/\partial E)|_{E_F}$ . Semi-quantitative agreement was obtained between calculated and experimental values of  $S$  at high temperatures, when this expression for  $S$  was applied to the calculated band structure of  $\text{Na}_x\text{CoO}_2$  [8]. However, the calculated  $N(E_F)$ , the electronic density of states (DOS) at the Fermi level, is unusually high for band metals. Also, the sublinearity of  $S(T)$  has been overlooked. Within the framework of the standard transport theory, this sublinearity may be accounted for by finite bandwidth and the corresponding temperature dependence of the chemical potential. The shift of  $\mu$  towards higher/lower energies for more/less than half filling, is accompanied by a widening of  $(-\partial f/\partial E)$ . For high enough temperatures, all states of a narrow band participate in conduction and  $S$  approaches saturation ( $S_{\text{sat}}$ ). It can be easily shown that in the atomic limit of a narrow band (for the Hubbard  $U \ll k_B T$  and two spin configurations per atomic state), equation (1) leads to  $S_{\text{sat}} = (k_B/|e|) \ln(n/(2-n))$ , where  $n$  is the number of electrons per atomic state and  $2-n$  the corresponding number of holes. Identifying the number of holes in  $\text{Na}_x\text{CoO}_2$  with  $1-x$ , the calculated  $S_{\text{sat}}$  for  $x = 0.6, 0.7$  are 119, 149  $\mu\text{V K}^{-1}$ , higher by less than 50% than  $S(\text{RT})$  measured on single crystals of similar compositions [2, 7, 13]. For  $x = 0.3$ ,  $S_{\text{sat}} = 53 \mu\text{V K}^{-1}$ , less than 50% higher than the experimental  $S_{\text{sat}}$  for our  $\text{Na}_x\text{CoO}_2 \cdot \gamma\text{H}_2\text{O}$  samples.

Magneto-thermopower measurements carried out on  $\text{Na}_x\text{CoO}_2$  showed that  $S$  is strongly suppressed by a magnetic field of 10 T [2]. This constitutes direct evidence for a large spin-entropy term in  $S$  implying that a strong-correlation picture is necessary to describe electronic transport in this material. The formula for  $S_{\text{sat}}$  for  $U \gg k_B T$  is [14, 15]:

$$S_{\text{sat}} = \frac{k_B}{|e|} \ln\left(b \frac{n}{1-n}\right) \quad (2)$$

where  $b$  is the spin degeneracy factor. In  $\text{Na}_x\text{CoO}_2$  the Co ions are in the low spin states of  $\text{Co}^{3+}$  and  $\text{Co}^{4+}$  ( $S = 1/2$  and  $S = 0$ , respectively). The concentration of  $\text{Co}^{3+}$  is  $x$ , that of  $\text{Co}^{4+}$ ,  $1-x$ . For  $b = 2$ , equation (2) yields  $S_{\text{sat}} = 94$  and  $132 \mu\text{V K}^{-1}$  for  $x = 0.6$  and  $0.7$ , respectively, close to the high  $T$  experimental values. However, unless the degeneracy of the  $\text{Co}^{3+}$  states is lifted, the dominant term in the low  $T$  thermopower is  $(k_B/|e|) \ln(b)$ ; for  $b = 2$ ,  $S \approx 60 \mu\text{V K}^{-1}$ . The degeneracy is lifted by spontaneous magnetic order or (in a paramagnetic state) by an applied magnetic field. The suppression of  $S$  ( $\text{Na}_x\text{CoO}_2$ ) by the magnetic field decreases with decreasing  $T$  below  $\theta$ , indicating a reduction of  $b$  from 2 to 1.

In the case of  $\text{Na}_x\text{CoO}_2 \cdot \gamma\text{H}_2\text{O}$  with  $n = x \approx 0.3$ , equation (2) predicts negative values of  $S_{\text{sat}}$  for either  $b = 1$  or 2. There are two possibilities:  $n > x$  if part of the water molecules are not inert or  $b > 2$ . The highest possible  $b$  for  $\text{Co}^{3+}$  (in the low spin state) is 6 [9]. For  $b = 4$  and  $n = 0.3$ , equation (2) predicts  $S_{\text{sat}} = 46 \mu\text{V K}^{-1}$ , very close to the observed saturation values.

We attempted to simulate the experimental  $S(T)$  for  $\text{Na}_x\text{CoO}_2$  and  $\text{Na}_x\text{CoO}_2 \cdot \gamma\text{H}_2\text{O}$  and to estimate the corresponding bandwidths using simplifying assumptions. We assumed  $N(E)$  ( $=1/W$ ) and  $\sigma(E)$  to be independent of energy. Equation (1) was modified, replacing the Fermi distribution function by  $f = (1 + b \exp(-\beta(\mu - E)))^{-1}$ , where  $\beta = (k_B T)^{-1}$  and  $b = 1 + a \exp(-\beta\Delta)$  with  $a = 1$  or 3.  $\mu(T)$  was calculated from  $n = (1/W) \int_0^W f(E) dE$  and  $S(T)$ , from the modified version of equation (1). In figure 3 the symbols represent the experimental data for the  $\text{Na}_x\text{CoO}_2$  and  $\text{Na}_x\text{CoO}_2 \cdot \gamma\text{H}_2\text{O}$  (B) samples; the solid curves through the data points represent the fitted theoretical curves, one for the upper data ( $a = 1$ ) and two for the lower data ( $a = 1$  and 3). The fitting parameters, are shown in table 1. The three lines fit very well the experimental data for the entire temperature range. The two low fitted curves differ slightly only at low temperatures (see inset of figure 3). Of the two possibilities for  $a$ ,

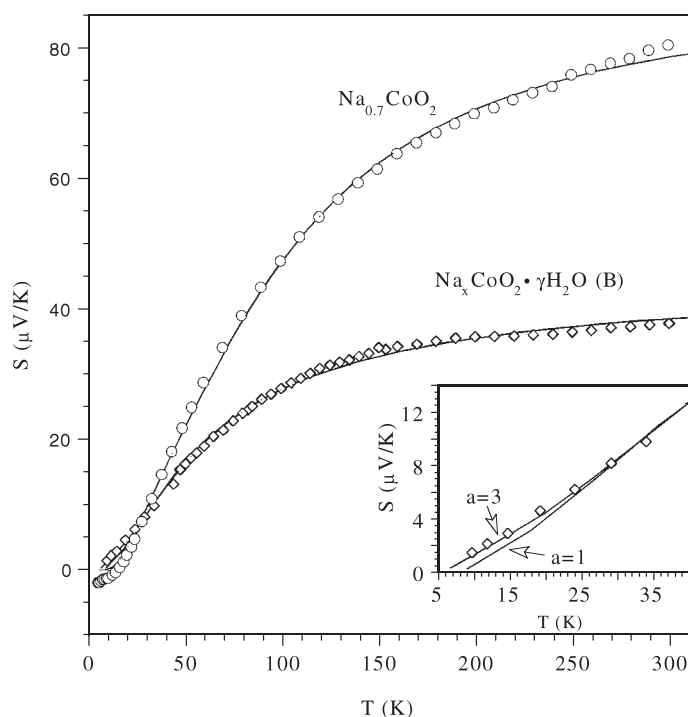


**Figure 3.** Calculated  $S(T)$  curves fitted to the experimental data of samples  $\text{Na}_{0.7}\text{CoO}_2$  and  $\text{Na}_x\text{CoO}_2 \cdot \gamma\text{H}_2\text{O}$  (B). Fitting parameters are listed in table 2. The lower portions of the plots for the hydrated compound are expanded in the inset. Note that the difference between the calculated curves for  $a = 1$  and 3 is visible only below 25 K.

**Table 2.**  $a$ , the parameter in the degeneracy factor  $b = 1 + ae^{-\beta\Delta}$  and parameters of the best fitted calculated  $S(T)$  curves (see figure 3).

| Sample   | $a$ | $n/\text{Co ion}$ | $\Delta/k_B$ (K) | $W/k_B$ (K)  |
|--|-----|-------------------|------------------|--------------|
| $\text{Na}_{0.7}\text{CoO}_2$                                | 1   | $0.591 \pm 0.001$ | $64 \pm 3$       | $757 \pm 22$ |
| $\text{Na}_x\text{CoO}_2 \cdot \gamma\text{H}_2\text{O}$ (B) | 1   | $0.457 \pm 0.002$ | $48 \pm 4$       | $178 \pm 22$ |
| $\text{Na}_x\text{CoO}_2 \cdot \gamma\text{H}_2\text{O}$ (B) | 3   | $0.297 \pm 0.001$ | $32.0 \pm 0.2$   | $132 \pm 4$  |

the agreement of the value of  $n$  ( $=0.297$ ) for  $\text{Na}_x\text{CoO}_2 \cdot \gamma\text{H}_2\text{O}$  (B) (see table 2) with  $x$  ( $\approx 0.31$ ) determined by EDS (see table 1) is remarkable for  $a = 3$ . For  $\text{Na}_x\text{CoO}_2$ , the corresponding  $n$  is 15% lower than the nominal  $x$ . In the bulk  $x$  may be lower than its nominal value (see footnote 2). Also, polycrystallinity may lead to slight reduction of  $S$  (corresponding to lower  $n$ ). Note that the fitted values of  $\Delta/k_B$  (see table 2) are close to  $\theta$  obtained from  $\chi(T)$  of  $\text{Na}_x\text{CoO}_2$  [2] and  $\text{Na}_x\text{CoO}_2 \cdot \gamma\text{H}_2\text{O}$  [5].

Band narrowing may be induced by the electron–electron interaction [16] or by the electron–phonon interaction [17]. In the latter case small polarons may form; at low enough temperature the motion of these heavy particles is coherent. There is evidence that polaron band narrowing also takes place in the Mott insulators<sup>4</sup>. The electron–phonon interaction may be dominant in the highly polarizable hydrated  $\text{Na}_x\text{CoO}_2$ . The roles of anisotropy and of carrier concentration in band narrowing may be separated by measurements of  $S(T)$  of  $\text{Na}_x\text{CoO}_2$  and

<sup>4</sup> See e.g. the conclusion section of [17].

$\text{Na}_x\text{CoO}_2 \cdot \gamma\text{H}_2\text{O}$  with identical  $x$ . This may lead to determination of the dominant interaction responsible for band narrowing.

In summary, the most remarkable result of this investigation is the band narrowing on going from  $\text{Na}_x\text{CoO}_2$  to  $\text{Na}_x\text{CoO}_2 \cdot \gamma\text{H}_2\text{O}$ ; it stands out from the experimental data, irrespective of interpretation. Theoretical simulation, based on transport by strongly correlated electrons, shows that  $W$  shrinks by a factor of 4–6. At low  $T$ , where superconductivity occurs, the relevant parameter is the enhanced DOS. The  $S(T)$  results are consistent with non-degenerate  $\text{Co}^{3+}$  states at  $T \rightarrow 0$  (implying an underlying order) and an increasing degeneracy with increasing  $T$ . Possible sources of band narrowing are briefly discussed.

We are grateful to Professor A Auerbach for kindling our interest in this new superconductor. KA is grateful for the support of a joint grant from the Center for Absorption in Science of the Ministry of Immigrant Absorption and the KAMEA Program.

## References

- [1] Terasaki I, Sasago Y and Uchinokura K 1997 *Phys. Rev. B* **56** R12685
- [2] Wang Y, Rogado N S, Cava R J and Ong N P 2003 *Nature* **423** 425
- [3] See: Motohashi T, Ueda R, Naujalis E, Tojo T, Terasaki I, Atake T, Karppinen M and Yamauchi H 2003 *Phys. Rev. B* **67** 64406
- [4] Takada K, Sakurai H, Takayama-Muromachi E, Izumi F, Dilanian R A and Sasaki T 2003 *Nature* **422** 53
- [5] Sakurai H, Takada K, Yoshii S, Sasaki T, Kindo K and Takayama-Muromachi E 2003 *Preprint cond-mat* 304503
- [6] Kawata T, Iguchi Y, Itoh T, Takahata K and Terasaki I 1999 *Phys. Rev. B* **60** 10584
- [7] Rivadulla F, Zhou J-S and Goodenough J B 2003 *Preprint cond-mat* 304455
- [8] Singh D J 2000 *Phys. Rev. B* **61** 13397
- [9] Koshibae W, Tsutsui K and Maekawa S 2000 *Phys. Rev. B* **62** 6869
- [10] Mott N F and Jones H 1936 *The Theory of the Properties of Metals and Alloys* (Oxford: Clarendon)
- [11] Ziman J M 1960 *Electrons and Phonons* (Oxford: Clarendon)
- [12] Blatt F J 1968 *Physics of Electronic Conduction in Metals* (New York: McGraw-Hill)
- [13] Terasaki I 2003 *Physica B* **328** 63
- [14] Heikes R R and Ure R W 1961 *Thermoelectricity* (New York: Interscience Publishers)
- [15] Beni G 1974 *Phys. Rev. B* **10** 2186
- [16] Ramakumar R, Jain K P, Kumar R and Chancey C C 1994 *Phys. Rev. B* **50** 10122 and references therein
- [17] Alexandrov A S and Mott Sir Nevill 1995 *Polarons and Bipolarons* (Singapore: World Scientific)